

ANIMAL PHYSIOLOGY

Whole-body endothermy in a mesopelagic fish, the opah, *Lampris guttatus*

Nicholas C. Wegner,^{1*} Owyn E. Snodgrass,² Heidi Dewar,¹ John R. Hyde¹

Endothermy (the metabolic production and retention of heat to warm body temperature above ambient) enhances physiological function, and whole-body endothermy generally sets mammals and birds apart from other animals. Here, we describe a whole-body form of endothermy in a fish, the opah (*Lampris guttatus*), that produces heat through the constant “flapping” of wing-like pectoral fins and minimizes heat loss through a series of counter-current heat exchangers within its gills. Unlike other fish, opah distribute warmed blood throughout the body, including to the heart, enhancing physiological performance and buffering internal organ function while foraging in the cold, nutrient-rich waters below the ocean thermocline.

The ability of an organism to conserve metabolic heat and maintain its body temperature above that of the surrounding environment (endothermy) increases reaction rates, muscle power output, and the capacity for sustained aerobic performance. This process provides distinct benefits, particularly for organisms that inhabit environments of low or variable temperature (1, 2). As such, endothermic organisms demonstrate a higher capacity for niche expansion and often gain a competitive advantage over organisms that thermoconform to their environment (such as in predator-prey interactions) (2–5). Because of the high heat capacity of water, the retention of body heat in aquatic habitats is extremely challenging, even for mammals, and thus only a small number of highly active fish species (<0.1% of described fishes) have acquired the ability to retain some internally produced heat (6–9). These fishes are termed “regional endotherms” because unlike mammals and birds, they

are only able to increase the temperature of specific tissues or organs.

The regionally endothermic tunas (family Scombridae) and lamnid sharks (family Lamnidae) (which warm their aerobic swimming musculature as well as other regions in some species) (6–12) and the billfishes (families Istiophoridae and Xiphiidae, which warm the eye and brain region only) (13, 14) are often termed “high-performance” fishes because of their increased physiological function associated with regional heat retention (8, 15). However, these fishes fall far short of whole-body endothermy because much of the body (including vital organs such as the heart) remains at ambient temperature, which ultimately puts limits on aerobic performance in cold water (16, 17). This limitation is linked to mechanisms used by these groups to reduce heat loss. Although conductive heat loss to the water is minimized by the location of heat-producing tissues near the body midline and insulation from the surrounding tissues, the main challenge to fish endothermy is the convective loss of heat as blood comes in close contact with the water at the gill lamellae (site of respiratory gas exchange). To reduce convective heat loss, these fishes have retia mirabilia or “wonderful nets” of blood vessels that form counter-current heat exchangers com-

posed of densely packed arterioles and venules running in opposing directions, in which warm venous blood returning from the heat-production site transfers its heat to the cold arterial blood arriving from the gills (18). To date, these retia in fish have only been observed in connection with specific muscle groups or organs, leaving the heart and many other tissues at ambient water temperature.

This study presents morphological, temperature, and behavioral data that demonstrate an independent evolution of a more whole-body form of endothermy present in the opah, *Lampris guttatus*—a poorly studied, large, mesopelagic fish with a circumglobal distribution. We show that unlike other fishes, the opah has putative heat-conserving retia located inside the gills, thus isolating the primary site of heat loss from the rest of the body. In situ temperature measurements acquired for freshly sacrificed opah landed during fisheries surveys reveal that the entire body core (pectoral swimming musculature, viscera, and heart) and cranial region (Table 1) are all significantly warmer than the environment. A representative superimposed thermal profile for a 40.0-kg opah reconstructed from more than 35 temperature measurements taken 4 to 5 cm beneath the skin over the entire animal (Fig. 1A) shows the general distribution of elevated temperatures. Elevated in situ temperatures were confirmed with in vivo measurements obtained by using a thermocouple implanted in the pectoral musculature of swimming opah released from our fishing vessel and tethered to a surface float for recapture. These fish had an average pectoral muscle temperature elevated $4.8 \pm 1.2^\circ\text{C}$ above ambient (Table 1) when swimming between depths of 50 to 300 m at water temperatures of 7.8 to 10.8°C (data for a 39.0-kg opah are shown in Fig. 1B).

In opah, the bulk of metabolic heat appears to be produced by the dark red aerobic pectoral musculature, which is used during continuous swimming (19) and is insulated from the water by a 0.88 ± 0.21 -cm-thick layer of fatty connective tissue (mean thickness \pm SD from 16 opah, 22.0 to 67.5 kg) (fig. S1). Unlike most fishes that use body undulation to achieve forward thrust during swimming, opah primarily use pectoral fin oscillation (movie S1). The aerobic pectoral musculature in opah comprises 16% of their total mass (37% of the total

¹Fisheries Resources Division, Southwest Fisheries Science Center, National Marine Fisheries Service (NMFS), National Oceanic and Atmospheric Administration (NOAA), La Jolla, CA 92037, USA. ²Ocean Associates, Southwest Fisheries Science Center, NMFS, NOAA, La Jolla, CA 92037, USA.

*Corresponding author. E-mail: nick.wegner@noaa.gov

Table 1. Regional body-temperature measurements (means \pm SD) taken from freshly captured and free-swimming opah.

Body region	Mean temperature (°C)	Temperature elevation above ambient (°C)	Number of fish (n)
In situ measurements (decked fish)			
Pectoral muscle	13.8 \pm 1.5	3.8 \pm 0.8	22
Cranial region	16.1 \pm 3.9	6.0 \pm 3.0	22
Viscera	13.5 \pm 1.6	3.5 \pm 1.0	21
Heart	13.2 \pm 1.7	3.2 \pm 0.7	19
In vivo measurements (free-swimming fish)			
Pectoral muscle	14.4 \pm 0.4	4.8 \pm 1.2	4

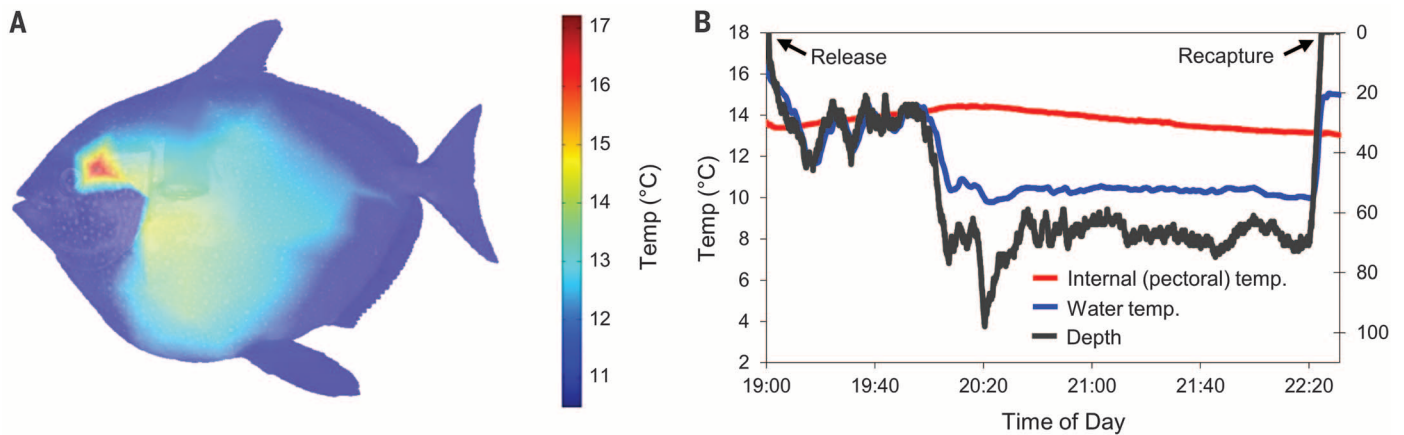


Fig. 1. Body temperature in the opah, *L. guttatus*. (A) In situ internal temperature profile (measurements taken ~4 to 5 cm below the skin) for a 98.0-cm fork length (40.0 kg) opah, with an ambient reference temperature of 10.5°C. (B) In vivo pectoral muscle temperature for a 96.4-cm (39.0 kg) opah swimming at depth.

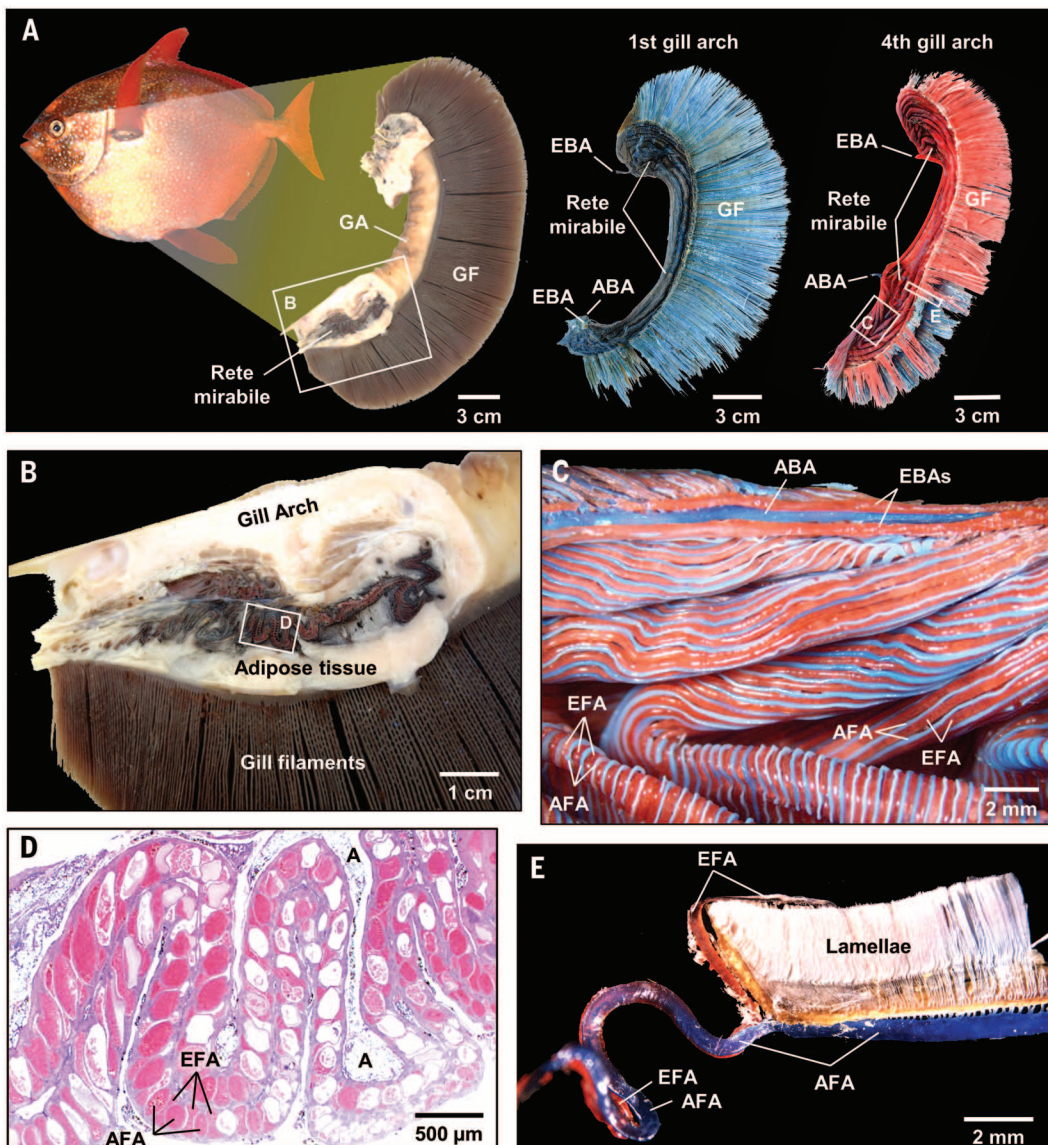


Fig. 2. Anatomy and vasculature of the opah gill. (A) Opah with enlarged fixed gill arch (left) and examples of vascular casts of the first gill arch (blue casting material only; center) and fourth arch (blue and red casting material; right). (B) Enlarged view of box “B” in (A) showing blood vessels of the rete mirabile surrounded by adipose tissue within the gill arch. (C) Enlarged view of box “C” in (A) showing the convoluted alternating afferent (blue, deoxygenated) and efferent (red, oxygenated) filament arteries forming the rete mirabile. (D) Magnified image of box in (B) showing a cross section through the rete with two rows of blood vessels (one associated with each gill hemibranch) containing alternating afferent and efferent filament arteries. (E) Gill filament extracted from box “E” in (A) showing the tight coupling of the afferent filament artery (blue, delivering deoxygenated blood to the gas-exchanging lamellae) with the efferent filament artery (red, returning with oxygenated blood). A, adipose tissue; ABA, afferent branchial artery; AFA, afferent filament artery; EBA, efferent branchial artery; EFA, efferent filament artery; GA, gill arch; GF, gill filaments.

propulsive musculature) (19), which is among the highest ratio reported for any fish and 25 to 800% more than that of the regionally endothermic tunas and lamnid sharks that warm their aerobic myotomal swimming musculature (table S1).

What is exceptional about the opah is its arrangement of counter-current retia mirabilia located inside each thick, fat-insulated gill arch (Fig. 2), which thermally isolate the respiratory exchange surfaces from the rest of the body. Vascular casts of the gills (Fig. 2, A, C, and E) reveal that unlike other fishes, extensions of the afferent and efferent filament arteries (which deliver and collect blood immediately pre- and post-gas exchange at the gill lamellae) are embedded within each gill arch in a tightly bundled and contorted manner to form an arterio-arterial rete. Specifically, the afferent and efferent arteries of each individual filament are closely coupled (Fig. 2E) and stacked in an alternating pattern within the arch (Fig. 2, C and D) so that the cold oxygenated blood of each efferent vessel (returning from the respiratory exchange surfaces) should be warmed by the conduction of heat from the warm deoxygenated blood in the afferent filament arteries on either side (which are carrying blood to the gas exchange surfaces). As a result, oxygenated blood leaving the respiratory exchange surfaces should be warmed before entering into efferent branchial arteries for distribution to the rest of the body.

Although these arterio-arterial retia should allow warm blood to be circulated throughout the body, the cranial region is warmer than the body core (Table 1 and Fig. 1), indicating an ad-

ditional heat source associated with the brain and extraocular muscles (the muscles that move the eye during swimming). Previous work suggests that heat may be produced by the proximal region of the paired lateral rectus muscles that attach at the base of the skull (immediately ventral to the brain) and conserved by small retia associated with the lateral and superior rectus muscles (20).

Of particular importance is the capacity of opah to increase the temperature of the heart, which receives warm blood from both the coronary arteries and the systemic venous return and is insulated from the opercular cavities by a 0.56 ± 0.07 -cm-thick fat layer (mean thickness from 15 opah, 22.0 to 67.5 kg). For the regionally endothermic tunas and lamnid sharks (which cannot warm the heart), both aerobic performance and foraging dives into cold water are thought to be largely limited by heart function, with weaker cardiac excitation-contraction (E-C) coupling leading to reduced cardiac outputs at lower temperatures (16, 17, 21, 22), which likely causes most species to return to surface waters to warm in between deep, cold water dives. Although some regionally endothermic species such as the salmon shark, *Lamna ditropis*, that spend considerable time in cold waters show enhanced expression of E-C coupling proteins to help mitigate the effect of low temperatures, cardiac function is still greatly reduced at colder temperatures (22). Evidence of an increased thermal tolerance in opah comes from satellite tracking data showing that opah spend most of their time below the mixed surface layer at depths between 50 and 400 m (Fig. 3)

(23) without regular visits to surface waters to warm.

With a warm body core and heart, and even warmer cranial region, opah have the capacity for enhanced physiological function in their deep, cold habitat. The elevated body temperature of opah should increase muscle power output and capacity for sustained performance, enhance temporal resolution and neural conductance for the eye and brain, increase the rates of food digestion and assimilation in the digestive tract, and reduce the impact of cold ambient temperatures and temperature changes on cardiac and other organ performance. Supporting its endothermic ability and increased aerobic performance, the opah has a relatively large heart and gill surface area, high hematocrit level, and an unusually large aerobic muscle mass (table S1), all of which are similar to characteristics of high-performance predators such as tunas and lamnid sharks, and in stark contrast to those of other fishes from its order (order Lampridiformes), which tend to be slow-moving ambush predators.

In many respects, the opah has converged with regionally endothermic fishes such as tunas and lamnid sharks for increased aerobic capacity. However, unlike these active, more surface-oriented predators that are thought to be derived from tropical ancestors and to use regional endothermy to expand their thermal tolerance or habitat utilization into deep and colder waters (6, 7), the opah's evolutionary history is likely tied to greater oceanic depths, with all but the most basal lineage of the Lampridiformes inhabiting the mesopelagic zone (200 to 1000 m depth) (24). Therefore, rather than using regional endothermy to dive below the thermocline during temporary forages, the opah (with its more whole-body form of endothermy) is distinctively specialized to exploit cold, deeper waters while maintaining elevated levels of physiological performance. The discovery of this form of endothermy, coupled with the recent finding of several distinct opah species inhabiting different regions of the world's oceans (25) (including the subpolar southern opah, *L. immaculatus*), sets the stage for future comparative studies to further explore this key evolutionary innovation.

REFERENCES AND NOTES

1. A. F. Bennett, *Am. J. Physiol.* **247**, R217-R229 (1984).
2. B. K. McNab, *The Physiological Ecology of Vertebrates: A View from Energetics* (Comstock, Ithaca, NY, 2002).
3. A. F. Bennett, J. A. Ruben, *Science* **206**, 649-654 (1979).
4. W. J. Hillenius, J. A. Ruben, *Physiol. Biochem. Zool.* **77**, 1019-1042 (2004).
5. J. Ruben, *Annu. Rev. Physiol.* **57**, 69-95 (1995).
6. K. A. Dickson, J. B. Graham, *Physiol. Biochem. Zool.* **77**, 998-1018 (2004).
7. B. A. Block, J. R. Finnerty, A. F. R. Stewart, J. Kidd, *Science* **260**, 210-214 (1993).
8. D. Bernal, K. A. Dickson, R. E. Shadwick, J. B. Graham, *Comp. Biochem. Physiol.* **129**, 695-726 (2001).
9. F. G. Carey, J. M. Teal, J. W. Kanwisher, K. D. Lawson, J. S. Beckett, *Am. Zool.* **11**, 137-145 (1971).
10. D. Bernal, J. M. Donley, R. E. Shadwick, D. A. Syme, *Nature* **437**, 1349-1352 (2005).

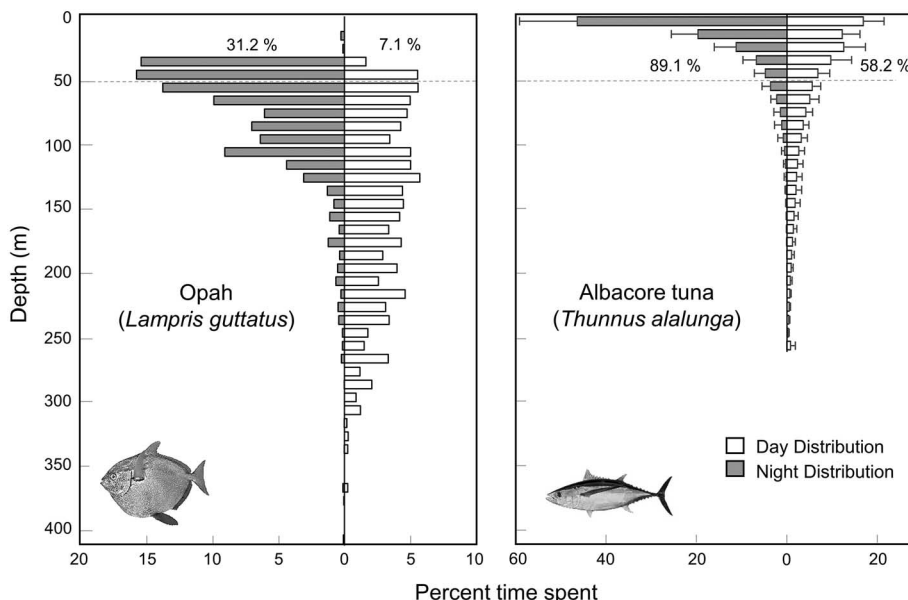


Fig. 3. Depth distribution of an opah in comparison with that of the regionally endothermic albacore tuna, *Thunnus alalunga*, as determined through archival tags. (Left) Opah. (Right) Albacore tuna. The percentage of time each species spent above 50 m (dotted gray line indicates the estimated mean depth of the bottom of the warm mixed surface layer) is shown for both daylight and nighttime hours. [Data for albacore tuna are from (26).]

11. J. M. Donley, C. A. Sepulveda, P. Konstantinidis, S. Gemballa, R. E. Shadwick, *Nature* **429**, 61–65 (2004).
12. J. B. Graham, K. A. Dickson, in *Tuna: Physiology, Ecology and Evolution*, B. A. Block, E. D. Stevens, Eds. (Academic Press, San Diego, CA, 2001), vol. 19, pp. 121–165.
13. B. A. Block, *J. Morphol.* **190**, 169–189 (1986).
14. F. G. Carey, *Science* **216**, 1327–1329 (1982).
15. R. W. Brill, *Comp. Biochem. Physiol.* **113**, 3–15 (1996).
16. H. A. Shiels, A. Di Maio, S. Thompson, B. A. Block, *Proc. Biol. Sci.* **278**, 18–27 (2011).
17. P. C. Castilho, A. M. Ladeira-Fernandez, J. Morrisette, B. A. Block, *Comp. Biochem. Physiol.* **148**, 124–132 (2007).
18. E. D. Stevens, in *Encyclopedia of Fish Physiology: From Genome to Environment*, A. P. Farrell, E. D. Stevens, J. J. Cech, J. G. Richards, Eds. (Academic Press, San Diego, CA, 2011), vol. 2, pp. 1119–1131.
19. R. H. Rosenblatt, G. D. Johnson, *Copeia* **1976**, 367–370 (1976).
20. R. M. Runcie, H. Dewar, D. R. Hawn, L. R. Frank, K. A. Dickson, *J. Exp. Biol.* **212**, 461–470 (2009).
21. J. M. Blank et al., *J. Exp. Biol.* **207**, 881–890 (2004).
22. K. C. Polovina et al., *Science* **310**, 104–106 (2005).
23. J. J. Polovina, D. Hawn, M. Abecassis, *Mar. Biol.* **153**, 257–267 (2008).
24. J. E. Olney, in *Species Identification Guide for Fisheries Purposes. Part 1 (Elopidae to Linophrynidae)*, K. E. Carpenter, V. H. Niem, Eds. (FAO, Rome, 1999), pp. 155–169.
25. J. R. Hyde, K. E. Underkoffler, M. A. Sundberg, *Mol. Ecol. Resour.* **14**, 1239–1247 (2014).
26. J. Childers, S. Snyder, S. Kohin, *Fish. Oceanogr.* **20**, 157–173 (2011).

ACKNOWLEDGMENTS

We thank H. Aryafar, S. Kohin, J. Renfree, R. Vetter, J. Wraith, and the crew of the M/V *Ventura II* for help with opah capture,

sampling, tagging, filming, and data visualization. We also thank C. Sepulveda for conversations and D. Bernal, R. Vetter, and R. Runcie for reviewing drafts of the manuscript. S. Snyder provided data from *T. alalunga*. We dedicate this paper to the late Dr. Jeffrey B. Graham, who spent much of his career studying regional endothermy in fishes and would have greatly enjoyed seeing this discovery. Data reported in this paper are archived at DOI: 10.5061/dryad.hq4v0.

SUPPLEMENTARY MATERIALS

www.sciencemag.org/content/348/6236/786/suppl/DC1
Materials and Methods
Figs. S1 and S2
Table S1
References (27–38)
Movie S1

10 February 2015; accepted 20 April 2015
10.1126/science.aaa8902

NEURODEVELOPMENT

Live imaging of adult neural stem cell behavior in the intact and injured zebrafish brain

Joana S. Barbosa,^{1,2} Rosario Sanchez-Gonzalez,¹ Rossella Di Giaimo,^{1,3}
Emily Violette Baumgart,¹ Fabian J. Theis,^{4,5} Magdalena Götz,^{1,6,7} Jovica Ninkovic^{1,6*}

Adult neural stem cells are the source for restoring injured brain tissue. We used repetitive imaging to follow single stem cells in the intact and injured adult zebrafish telencephalon *in vivo* and found that neurons are generated by both direct conversions of stem cells into postmitotic neurons and via intermediate progenitors amplifying the neuronal output. We observed an imbalance of direct conversion consuming the stem cells and asymmetric and symmetric self-renewing divisions, leading to depletion of stem cells over time. After brain injury, neuronal progenitors are recruited to the injury site. These progenitors are generated by symmetric divisions that deplete the pool of stem cells, a mode of neurogenesis absent in the intact telencephalon. Our analysis revealed changes in the behavior of stem cells underlying generation of additional neurons during regeneration.

The maintenance of adult neural stem cells (aNSCs) is important for life-long organ homeostasis (1) and regeneration (2–4). There is presently a discrepancy between models describing the behavior of aNSCs in the mammalian brain, one proposing largely depletion of aNSCs (5, 6) and the other some degree of long-term self-renewal (7). In the adult zebrafish brain, aNSCs exist not only in a more widespread manner compared with those of mammals but also react to injury by regenerating neurons (2, 3, 8–14). Indeed, the cellular architecture is restored, which includes additional neurogenesis

after stab wound injury in the adult zebrafish telencephalon (2, 3, 11, 13, 14). As aNSCs are positioned close to the surface in the zebrafish dorsal telencephalon (12, 15) (Fig. 1A), the behavior of aNSCs in the intact brain and during regeneration of the injured brain can be examined non-invasively by live *in vivo* imaging.

We established a protocol by which we could follow individual aNSCs over time [fig. S1A and supplementary materials (SM)]. We used the *brassy* zebrafish line, which has low pigment levels, crossed with the *Tg(gfap:GFP)mi2001* transgenic line (16), which labeled aNSCs (Fig. 1A). We sparsely labeled the glial fibrillary acidic protein promoter–driven green fluorescent protein (*gfap:GFP*)–positive aNSCs (see SM) by electroporation of plasmids encoding for red fluorescent proteins [tdTomato, mCherry, or red fluorescent protein (RFP)] (fig. S1 and SM). Most of the labeled cells with radial morphology were immunoreactive to GFAP (106 of 124 cells; 85%) (fig. S1, E and F) and did not differ with regard to their proliferation from the overall *gfap:GFP*–positive aNSCs (fig. S1, C and D). Individual tdTomato-labeled NSCs at the

dorsal brain surface were identified by their position relative to the stable *gfap:GFP*–positive cells (colored dots in Fig. 1C). These individual cells were then followed by imaging through the thinned skull for a period of 1 month (fig. S1A). As many reporter-positive cells neither moved nor divided, we used their distribution pattern in post-imaging immunostaining and microscopy to re-identify and confirm cell identity of imaged cells (figs. S2, S4, and S5).

In the intact brain, aNSCs rarely divide (17, 18). Indeed, 66 of 109 (61%) of the labeled aNSCs in the intact zebrafish telencephalon stayed quiescent without changing their identity throughout the imaging time (fig. S2), and only 1 of 109 cells followed by live imaging died. However, 14 aNSCs (13%, $n = 109$) divided during this time. We found that the aNSCs rarely divided symmetrically (1 cell of 109; 0.9%) (Fig. 1C; fig. S3, B and E; fig. S4; and movies S1 and S2), with one aNSC generating two aNSCs, both of which retained *gfap:GFP* expression and the characteristic thick radial process (fig. S4). In contrast, 13 of 14 dividing aNSCs (~93%) divided asymmetrically, generating one cell with aNSC identity (radial morphology and *gfap:GFP* expression) and one cell that lacked the radial morphology (Fig. 2; fig. S3, B and E; figs. S5 and S6; and movies S3 and S4). Of these progeny lacking radial morphology, 25% (two of eight cells) also lost *gfap:GFP* expression (GFP-negative progeny in fig. S3, B and D). Because GFP is very stable, the protein can persist even after the cell is no longer an aNSC (Fig. 1B), and some GFP-positive cells do not express aNSC markers (15). Although asymmetrically generated daughter cells differ in regard to inheritance of GFP, all of them lose the radial glia morphology, the defining criteria for the asymmetric divisions (93%, 13 of 14 dividing aNSCs). Some cells that had lost the radial process, however, were not immunoreactive for the neuronal marker HuC/D (figs. S3B and S5C), which implies that they may be intermediate progenitor cells.

To examine the behavior of Sox2-positive intermediate progenitors (fig. S7), we used Moloney murine leukemia virus–based retroviral vectors to stably transduce progenitor cells (18). We analyzed their clonal progeny that contained no glia

¹Institute of Stem Cell Research, Helmholtz Center Munich, Munich, Germany. ²Ph.D. Program in Biomedicine and Experimental Biology (BEB), Center for Neuroscience and Cell Biology, University of Coimbra, Coimbra, Portugal. ³Department of Biology, University of Naples Federico II, Naples, Italy. ⁴Institute of Computational Biology, Helmholtz Center Munich, Munich, Germany. ⁵Institute for Mathematical Sciences, Technical University Munich, Garching, Germany. ⁶Biomedical Center, University of Munich, Munich, Germany. ⁷Munich Cluster for Systems Neurology “SyNergy,” Ludwig Maximilian University of Munich, Munich, Germany.
*Corresponding author. E-mail: ninkovic@helmholtz-muenchen.de

This copy is for your personal, non-commercial use only.

If you wish to distribute this article to others, you can order high-quality copies for your colleagues, clients, or customers by [clicking here](#).

Permission to republish or repurpose articles or portions of articles can be obtained by following the guidelines [here](#).

The following resources related to this article are available online at www.sciencemag.org (this information is current as of May 14, 2015):

Updated information and services, including high-resolution figures, can be found in the online version of this article at:

<http://www.sciencemag.org/content/348/6236/786.full.html>

Supporting Online Material can be found at:

<http://www.sciencemag.org/content/suppl/2015/05/13/348.6236.786.DC1.html>

This article **cites 31 articles**, 11 of which can be accessed free:

<http://www.sciencemag.org/content/348/6236/786.full.html#ref-list-1>

This article appears in the following **subject collections**:

Anatomy, Morphology, Biomechanics

http://www.sciencemag.org/cgi/collection/anat_morp